Pakistan J. Zool., pp 1-13, 2023. **DOI**: https://dx.doi.org/10.17582/journal.pjz/20230512070544

Modulation of Tau Expression in the Colonic Muscle Layer of a Rat Model with Opioid-Induced Constipation

Jinzhao Li[1], Yawen Zhang[2], Binghan Jia[1], Yuqiong Zhao[1], Huijuan Luo[1], Xiaojie Ren[1], Yuan Li[3], Xiaoyan Bai[1], Jing Ye[3] and Junping Li[1]*

[1]Department of College of Basic Medical Sciences, Ningxia Medical University, No. 1160 of Shengli Street, Ningxia Hui Autonomous Region, Yinchuan 750004, China
[2]Department of General Surgery, People's Hospital of Ningxia Hui Autonomous Region, Yinchuan 750004, China
[3]Department of College of Clinical Medicine, Ningxia Medical University, Yinchuan 750004, China

Jinzhao Li and Yawen Zhang contributed equally to this study.

Article Information
Received 12 May 2023
Revised 03 August 2023
Accepted 18 August 2023
Available online 17 November 2023 (early access)

Authors' Contribution
Conception and design of the study: JZL, YWZ, YQZ and JPL. Preparation of animal models and experiments: JZL, YWZ, BHJ, HJL, XJR, YL, QW, XYB and JY. Data analysis: JZL, YWZ and BHJ. Supervision: JZL, YWZ. Drafting the manuscript: JZL, YWZ, YQZ and JPL. Critical revision of the manuscript: JZL, YWZ and LJ. Approval of the final manuscript: All authors.

Key words
Tau, μ-opioid receptor (MOR), Opioid-induced constipation (OIC), Colon, Intestinal muscle plexus

ABSTRACT

The main objective of this study was observe the distribution and expression of tau in the distal colonic muscle layers using opioid-induced constipation (OIC) rat model and to explore the mechanistic correlation between the tau phosphorylation and occurrence of OIC. The rat model of OIC was generated by intraperitoneal (i.p) injection of loperamide hydrochloride (Lop; 5mg/kg), and was evaluated by examining the fecal properties, intestinal propulsion mobility, immunohistochemistry (IHC), western blot (WB) and ELISA for detecting levels of Tau, P-Ser396-tau, P-Ser404-tau, protein kinase C (PKC), p38 MAPK (p38), p-p38 MAPK (p-p38) and μ-opioid receptors (MORs) in the colonic samples. The gene sequencing approach was used to detect alternatively spliced tau isoforms in the distal colonic muscle layer. Sequencing analysis revealed that 3 isoforms of tau, namely 2N4R, 1N4R and 0N4R were expressed in the distal colonic myocardium tissue. OIC rats had small, dry and hard feces, and intestinal propulsion velocity was significantly slower, especially in the distal colon. P-Ser396-Tau, P-Ser404-Tau, PKC, p-p38, p38, and Tau positive cells were distributed in the intestinal muscle plexus of the distal colon, and all of them were colocalized with MORs; though the expressions levels of tau and p38 remained unchanged, others indexes above significantly increased in the distal colonic muscle layer of OIC rats. However, after the administration of p38 blocker SB203580, OIC rats had salami-like feces, with an increase in colonic propulsion velocities; although the expressions levels of Tau and p38 didn't change significantly in distal colonic muscle layers, the expressions levels of P-Ser396-Tau, P-Ser404-Tau, and p-p38 significantly reduced. To conclude there is a unique distribution pattern of tau within the distal colonic musculature of OIC rats. The abnormal activation of MORs contributes to the hyperphosphorylation of tau protein, which in turn induces the development of OIC.

INTRODUCTION

Opioids, such as morphine, are powerful and effective analgesics commonly used in clinical practices for relieving intractable pain. However, long-term opioid treatment can have serious gastrointestinal (GI) disorders, especially constipation (Porta-Sales *et al*., 2015; Guerrero-Alba *et al*., 2017). The main reason is that opioid weakens the secretion of gastrointestinal epithelial cells, slows down gastrointestinal peristalsis, and excessive absorption of water by the intestinal mucosa, leading to symptoms such as constipation (Porta-Sales *et al*., 2015). Statistically, about 80-90% of cancer patients develop serious constipation symptoms after receiving opioid medications for a longer duration. Some patients eventually have to discontinue taking these drugs because they cannot tolerate the constipation-associated pain (Farmer *et al*., 2018), which greatly impacts the analgesic's clinical benefits.

* Corresponding author: lijunping_jp@163.com
0030-9923/2023/0001-0001 $ 9.00/0

It is demonstrated that opioids exert analgesic effects in the central nervous system (CNS), while long-term medication-induced GI dysfunctions are primarily associated with the peripheral nerves (Guerrero-Alba *et al*., 2017; Luo *et al*., 2011). In the GI tract, the main site of the action of opioids is μ-opioid receptors (MORs) on the surface of enteric nerve cells (Galligan and Sternini, 2017), where it mediates the release of inhibitory neurotransmitters (Wang, 2021), thereby inhibiting the transport function of the GI tract, and retaining food contents in the intestinal lumen for long to be dehydrated, leading to constipation. After knocking out the MOR gene in mice, the gastrointestinal motility disorders caused by opioids disappear (Galligan and Akbarali, 2014). However, the MOR-mediated signaling pathways and molecular mechanisms that regulate the release of inhibitory neurotransmitters from colonic nerve cells are still unclear.

Moreover, it is shown that long-term opioid administration can induce hyperphosphorylation of tau in brain cells (Ohene-Nyako *et al*., 2021). Tau, a microtubule-associated protein, is predominantly expressed in neurons in the CNS, maintaining microtubule stability and assisting axonal transport. Under pathological conditions, hyperphosphorylated tau disturbs the microtubule stability and induces axonal transport dysfunction, thus affecting neurotransmitter release (Lauretti and Praticò, 2020; Zhang *et al*., 2018). It has been reported that tramadol, a very well-tolerated opioid analgesic, could ameliorate pathological conditions in Alzheimer's disease via inhibiting mTOR and hence activating tau dephosphorylation and autophagy respectively (Pourtalebi *et al*., 2018). But the administration of the MOR antagonist Naloxone can inhibit Tau hyperphosphorylation, which is similar in effect to the protein kinase p38 inhibitor SB203580 (Ramage *et al*., 2005; Cao *et al*., 2013). However, there is uncertain whether tau phosphorylation signaling pathway is involved in the process of constipation caused by long-term opioid treatment.

At present, most of the studies on the pathological mechanism of Tau focus on degenerative disease. However, there are few studies on Tau's peripheral nervous system, especially on gastrointestinal Enteric nervous system diseases. Putting all these connections together, it could be hypothesized that constipation caused by the long-term administration of opioids is associated with the interactions between the tau phosphorylation signaling pathways and MORs in enteric nerve cells, leading to nerve cell dysfunctions. Therefore, we aim to investigate the distribution characteristics of tau in the distal colon muscle layers of rats with the opioid-induced constipation (OIC) by using intestinal function tests, immunohistochemistry (IHC) and western blot assays.

Therefore, we proposed to establish a rat constipation model using loperamide hydrochloride (Lop), a selective agonist of the MOR, to investigate the distribution characteristics of tau in the distal colon muscle layers of rats with the opioid-induced constipation (OIC) by using intestinal function tests, immunohistochemistry (IHC) and western blot assays.

MATERIALS AND METHODS

Animals

Male Sprague-Dawley rats (Laboratory Animal Center of Ningxia Medical University, Certificate of Conformity No. SCXK (Ning) 2020-0001) of 180-220 g were purchased and housed in a specific pathogen-free (SPF) environment at about 23°C room temperature and 60% of humidity.

Reagents

Lop capsules (Xi'an Janssen Pharmaceutical), the MOR antagonist naloxone hydrochloride (APExBIO), p38 MAPK agonist anisomycin (ANS), p38 MAPK blocker SB203580 (MedChemExpress) and India ink (Bioss) were purchased from the respective companies. The following primary antibodies were used in this study: Anti-tau rabbit pAb (ABclonal), anti-phospho-tau (Ser396), anti-MOR guineapig pAb (Novus), anti-phospho-tau (Ser404) rabbit mAb, anti-p38-MAPK rabbit mAb, anti-phospho-p38-MAPK rabbit mAb (Cell Signaling Technology), anti-PKC rabbit mAb, anti-MOR rabbit pAb, anti-NeuN mouse mAb (Abcam), anti-βTubulin mouse mAb and anti-β-actin mouse mAb (zsbio). Goat anti-rabbit IgG HandL (Alexa-Fluor488), goat anti-rabbit IgG H and L (Alexa-Fluor594) and goat anti-guineapig IgG H and L (Alexa-Fluor488) secondary antibodies were obtained from Abcam). The horseradish peroxidase (HRP)-conjugated goat anti-mouse IgG and goat anti-rabbit IgG were purchased from zsbio.

Preparation of models and groups

Rats were randomly divided into the normal control group (NCG), the normal saline group (NSG), and The OIC group, with twenty mice in each group. The NCG rats were not given any treatments. Rats in the NSG were given 0.9% of NaCl solution intraperitoneally at 2 mL/time and 2 times/day for 7 consecutive days, while rats in the OIC group rats were administered a 5mg/kg Lop suspension intraperitoneally at 2 mL/time and 2 times/day for 7 consecutive days (Huang *et al*., 2020; Ma *et al*., 2021).

On the 8th day, the OIC rats were divided into 4 groups: the OIC + SB203580 group, the OIC + ANS group,

the OIC + Naloxone group, and the OIC + NaCl group, which were injected with SB203580 solution, anisomycin solution, naloxone solution and 0.9% of NaCl solution, respectively. Each group was continuously injected for 4 days, once a day (5 mg/kg, 2 mL/time).

Evaluation of the constipation rat model

(i) *Body weight:* The body weight of each rat was measured and recorded before dosing from day 1 of the modeling.

(ii) *Fecal traits and grade scoring:* Fecal traits of rats were examined and recorded daily from the first day of modeling. The feces were graded according to the Bristol stool trait criteria (Young *et al*., 2018): Grade I for the discrete hard lumps; grade II for the small bologna-like lumps; grade III for Weenie-like with cracks on the surface; grade IV for the Weenie-like but smooth and soft; grade V for the soft lumpy but with clear borders; grade VI for paste-like and unclear boundary; and grade VII for watery appearance. Furthermore, grades I-II referred to constipation, grades III-IV for normal, and grades V-VII for diarrhea symptoms.

(iii) *Intestinal propulsion velocity (IPV):* After establishing the constipation model, rats were distributed in three groups and gavaged with 2 mL of Indian ink through the mouth without food. On the 4th day of drug intervention, the rate of colonic IPV was calculated. Rats were sacrificed at different time points after 12h of gavage, then the entire intestines, from the pylorus to the rectum, were harvested. The rectum was pulled under no tension, and the distances of ink propulsion in the small intestine and proximal, middle and distal colons were measured separately. The time required for ink propulsion in each group of rats was recorded. The distance advanced was divided by the time to calculate the velocity of ink propulsion, and statistical analysis was performed.

IHC

NCG rats were selected and fixed on a dissection table following deep anesthesia with isoflurane by inhalation. Then the intestine was properly exposed by cutting along the midline of the abdomen, and the distal colon was harvested. The intestinal canal was flushed, and one end of the canal was ligated. The intestinal canal was filled with tissue fixative until the intestinal wall was stretched, and the other end of the canal was quickly ligated. The intestinal tube was fixed in a fixative solution for 8h, then transferred to a 30% sucrose solution for 12h. The intestinal tube was then removed, cut along the mesentery, and placed in a fresh 30% sucrose solution for further dehydration. After dehydration was completed, the mucosal, submucosal, and circular muscle layers were peeled off, and the longitudinal muscle layer was retained. An appropriate amount of tissue sample was taken from the longitudinal muscle layer and rinsed thrice with PBS. The tissue samples were then repaired with diluted hydrochloric acid for 60min, followed by incubation in goat serum for 70min. The following primary antibodies were added at the indicated dilutions: Anti-Tau, anti-P-Ser396-Tau, anti-P-Ser404-Tau, anti-PKC, anti-p38, anti-p-p38, anti-NeuN and anti-MOR (all 1:150), for 1h at room temperature, then placed in the refrigerator at 4°C for 54h. After incubation, samples were washed with PBS. Then samples were incubated with respective secondary antibodies for 2h at room temperature and washed with PBS. The slices were sealed with a fluorescent blocker, observed under the microscope, and photographed.

Full length transcriptome sequencing

NCG, NSG and OIC rats were selected, deeply anesthetized with isoflurane, fixed on a dissection table, and the intestine was properly exposed by cutting along the midline of the abdomen to harvest the distal segment of the colon. The mucosal and submucosal layers were peeled off, and the intestinal muscle layer tissues were preserved. Nucleic acid extraction was completed using cassette/TRIzol reagent, concentrations were measured using Nanodrop2000, and the DNA integrity was tested by Agient2100, LabChip GX, and agarose gel mapping. Flow cell priming mix was prepared using the sequencing chip preparation kit (EXP-FLP001 PRO.6), and the upload library was configured by the ligation sequencing kit (SQK-LSK109). The MinKnow software was run on the PromethION48 sequencer with the PromethION Flow Cells (FLO-PRO002) chip. The sequencing reaction was run for 72h by default. The gene sequencing experiment was conducted by Biomarker technologies CO., LTD (Münster, Germany), depicted in Supplementary Material 1.

The enzyme-linked immunosorbent assay (ELISA)

NCG, NSG and OIC rats distal colon muscle tissues were collected and homogenized in PBS buffer, centrifuged for 5min at 12000g at 4°C in a high-speed refrigerated centrifuge, and the supernatant was collected in a new tube. Standards were diluted according to the instructions, samples were added to it, and incubated for 30 min at a 37°C thermostat. After that, the liquid was discarded, washing solutions were added, and allowed to stand for the 30s. The enzyme reagent was subsequently added to the reaction mix and incubated at 37℃ for 30 min. The samples were washed again, chromogenic agents A and B were added, and incubated for 10 min at 37°C. The reaction was terminated by adding termination solution, and the absorbance (OD) was measured. The concentrations of the

standard were used as the horizontal coordinates and the OD values as the vertical coordinates to draw the standard curve. The linear regression equation was applied to calculate the concentration of the respective samples from the standard curve and multiplied by the dilution factor to determine the actual concentration of the sample.

Western blot

Harvested tissue samples of the distal colonic muscle layer from NCG, NSG and OIC rats were used for protein extraction using a commercial protein extraction kit. The protein concentration was determined by the BCA method. Protein samples were resolved on 10% SDS-PAGE, followed by transfer on the membrane. The membrane was blocked by incubating in non-fat 5% skim milk for 4h at room temperature, before adding the following primary antibodies: anti-Tau, anti-P-Ser396-Tau, anti-P-Ser404-Tau, anti-MOR, anti-PKC, anti-β-actin, anti-p38, anti-p-p38 and anti-β-tubulin (all 1:1000), with another incubation in the refrigerator at 4°C for 16h. After that, TBST was used to wash thrice to clear off any unbound primary antibodies, then incubated with the corresponding secondary antibodies (1:4000) for 1h at room temperature, and washed with TBST. The ECL reagent was added, and the images were captured by a chemical imaging system (Amersham Image 600). The gray value of each band was determined using ImageJ software and compared to the relative internal reference bands (target protein gray value/ internal reference protein gray value).

Statistical analysis

In the process of measurements and observations, double-blind approach was adopted to ensure that the results were not influenced by subjective factors. This study used the SPSS Statistics (V.24.0, IBM) software to conduct statistical analysis. Measurement data that obeyed normal distribution were described by mean ± standard deviation, and a one-way analysis of variance was used for comparison between multiple groups. Measurement data that did not obey normal distribution were described by median and interquartile spacing, and a Kruskal–Wallis H rank-sum test was used for comparison between multiple groups. Paired samples were compared using a Wilcoxon rank-sum test, while a frequency was used to describe the count data. The chi-square test or Fisher's exact probability method was used to analyze the distribution differences, and $P<0.05$ was considered statistically significant.

RESULTS

Effect of OIC on body weight, fecal grade scores, and IPVs of rats

During the modeling period, OIC rats gained weight at a significantly slower rate, about 2 g per day, while NSG and NCG rats gained about 10g per day (Fig. 1A).

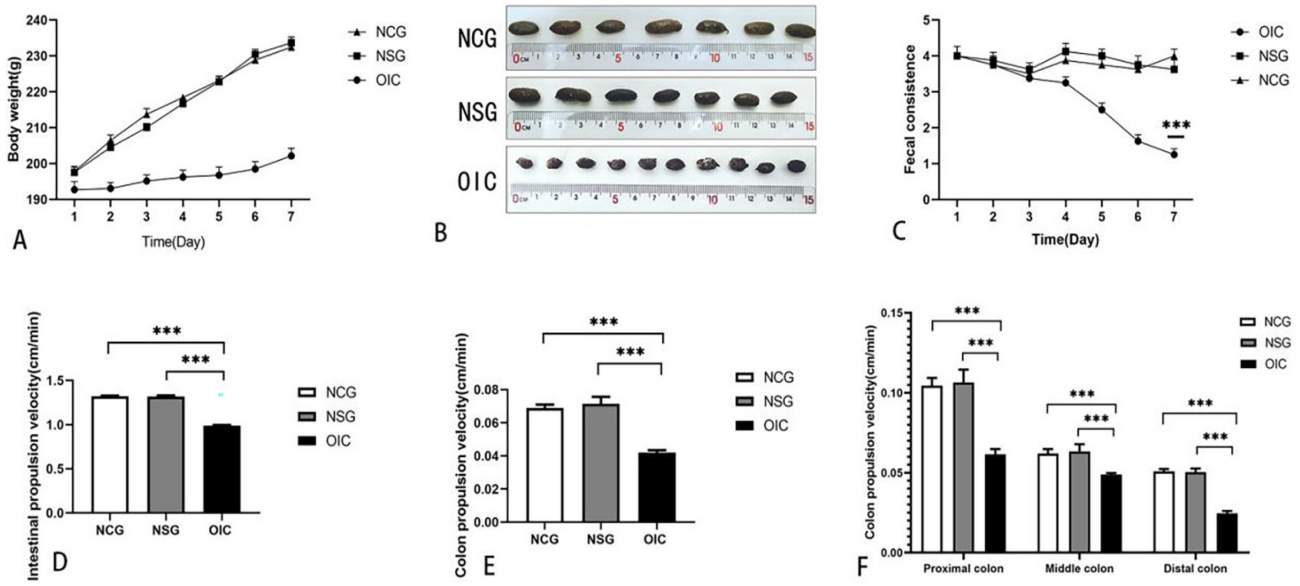

Fig. 1. Body weight, fecal grade scores and intestinal propulsion velocities of rats in the 3 groups were estimated. **A,** Changes in body weight of rats in the 3 groups. **B,** Fecal traits of rats in the 3 groups. **C,** Fecal trait grade scores of rats in the 3 groups. **D-F,** Comparison of intestine propulsion velocity.

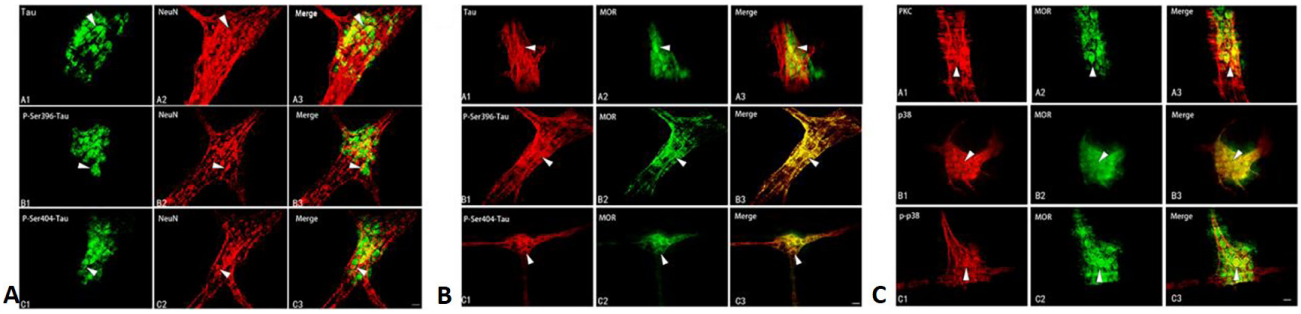

Fig. 2. Immunohistochemistry of the colonic myenteric plexus tissues from normal rats. **A, (**A1) Tau-positive cells; (A2) NeuN-positive cells; (A3) Intracellular co-expressions of Tau and NeuN. (B1) P-Ser396-Tau-positive cells; (B2) NeuN-positive cells; (B3) Intracellular co-expressions of P-Ser396-Tau and NeuN. (C1) P-Ser404-Tau-positive cells; (C2) NeuN-positive cells; (C3) Intracellular co-expressions of P-Ser404-Tau and NeuN. **B,** (A1) Tau-positive cells; (A2) MOR-positive cells; (A3) Co-expressions of Tau and MOR markers in enteric neural cells. (B1) P-Ser396-Tau-positive cells; (B2) MOR-positive cells; (B3) Co-expressions of P-Ser396-Tau and MOR in enteric nerve cells. (C1) P-Ser404-Tau-positive cells; (C2) MOR-positive cells; (C3) P-Ser404-Tau and MOR double-positive enteric nerve cells. **C,** (A1) PKC-positive cells; (A2) MOR-positive cells; (A3) Co-expressions of PKC and MOR in enteric nerve cells. (B1) P38-positive cells; (B2) MOR-positive cells; (B3) Co-expressions of p38 and MOR in enteric nerve cells. (C1) P-p38-positive cells; **(**C2) MOR-positive cells; (C3) Co-expressions of p-p38 and MOR in enteric nerve cells. Scale bars: 20μm.

As the modeling time progressed, the stool of OIC rats gradually became harder and smaller. On the 7th day, the surface was cracked or in scattered pieces, whereas NSG and NCG rats had smooth, soft, and salami-like stool surfaces (Fig. 1B). According to the Bristol stool trait scoring, on the 7th day of modeling, the OIC rats' fecal grade score was approximately Ⅰ, but the NSG and NCG rats reached a grade of IV. There were significant differences between the OIC, NSG, and NCG rats' fecal grading scores (***P<0.001, Fig. 1C).

After oral gavage of Indian ink, the duration of the ink to be expelled from the small intestine took about 2h for OIC rats, while 1.5h for both NSG and NCG rats, respectively. Whereas the travel time of the ink from the ileocecal opening to the end of the proximal colon was about 1.5h for OIC rats and 1h for both NSG and NCG rats. From the right flexure of the colon to the end of the middle colon, the ink travel time was about 2h for OIC rats and 1.5h for both NSG and NCG rats. Pushing the ink from the left flexure of the colon to the end of the distal colon took about 4h for OIC rats and 2h for both NSG and NCG rats. The discharge of ink from the small intestine to the end of the distal colon took about 7.5h for OIC rats and 4.5h for both NSG and NCG rats. In OIC rats, the dye movement velocity was significantly slower compared with that of NSG and NCG rats in terms of small intestinal propulsion velocity (***P<0.001, Fig. 1D). Likewise, the colonic propulsion was significantly slower in OIC animals compared with that of NSG and NCG rats (***P<0.001, Fig. 1E). Similarly, the proximal, middle and distal colonic propulsions, especially the distal colonic propulsion, were drastically slower in OIC rats than that in NSG and NCG animals (***P<0.001, Fig. 1F).

Distribution of Tau, P-Ser396-Tau, P-Ser404-Tau, PKC, p38, p-p38 and MOR in the colonic myenteric plexus

IHC assay revealed expressions of positive markers like Tau, P-Ser396-Tau and P-Ser404-Tau in the rat distal colonic myenteric plexus, with the positive markers located mainly in the cytoplasm, with round or ovoid shapes and short protrusions. The positive markers were all co-expressed with NeuN, suggesting that these positive cells were neurons (Fig. 2A). Amongst the positive cells, Tau and MOR double-positive nerve cells were oval in shape, having marker expressions mainly in the cytoplasm. These markers were also found to form clusters into ganglia, with nerve fibers crossing from the ganglia. The P-Ser396-Tau and P-Ser404-Tau double-positive nerve cells were round or oval in shape, and positive markers were mainly located in the cytoplasm. Several protrusions emanated from the cytosol of these cells, with only one longer protrusion (Fig. 2B). P38 and MOR double-positive nerve cells were round or oval in shape. The markers were expressed in the cytoplasm and found to cluster in ganglia with nerve fibers crossing from the ganglia. Interestingly, PKC and p-p38 positive nerve cells were round or oval in shape, and the positive markers were mainly located in the cytoplasm with several protrusions from the cytosol (Fig. 2C).

Expressions of tau isoforms in the rat distal colonic muscular layers.

Full length transcriptome sequencing results revealed

that seven tau-related mRNA transcripts were expressed after selective splicing of the MAPT gene in the distal colonic muscular layers and three tau isoforms, 2N4R, 1N4R, and 0N4R were expressed post-translationally. Among them, ENSRNOT00000042984 contained only the exon10, expressing the 0N4R isoform. ENSRNOT00000045127 included exon2, exon3 and exon10, expressing the 0N4R isoform after translation. ENSRNOT00000045127 included exon2, exon3 and exon10 and expressed the 2N4R isoform. In NSRNOT00000050070 and ONT.4179.3, exon10 was present, expressing 0N4R isoform. In both ONT.4179.1 and ONT.4179.2, exon3 and exon10 were present, post-translationally expressing the 1N4R isoform (Fig. 3A). Expressions of ENSRNOT00000006947, ENSRNOT00000050070, ONT.4179.2 and ONT.4179.3 isoforms were determined in the myenteric layer of the rat colon. Statistical analysis showed that there were no significant differences in the expressions of the 7 mRNAs within the colonic myenteric layers of rats in the three groups of OIC, NSG and NCG (Fig. 3B).

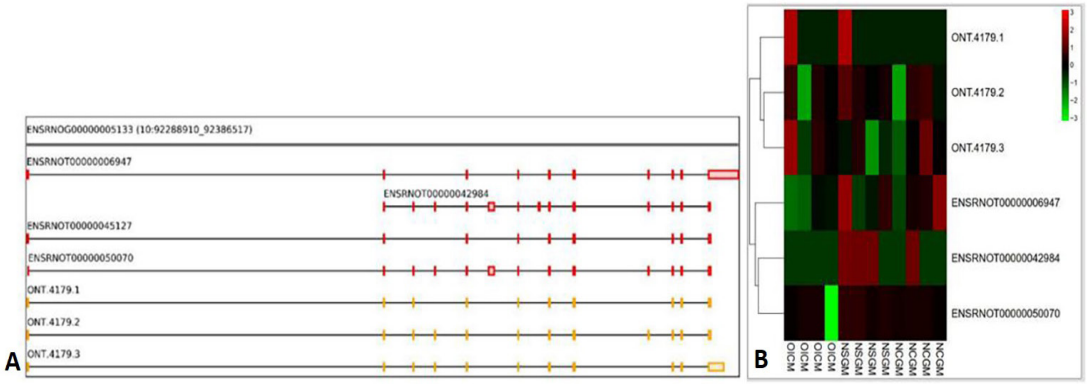

Fig. 3. Gene sequencing analysis of the distal colonic myometrium tissues of the three groups of rats 7 days after modeling. A, Selective splicing events of MAPT gene, expressing different isoforms of tau. B, No significant differences in tau-related mRNA expressions were observed in OIC rats compared with that of NCG and NSG.

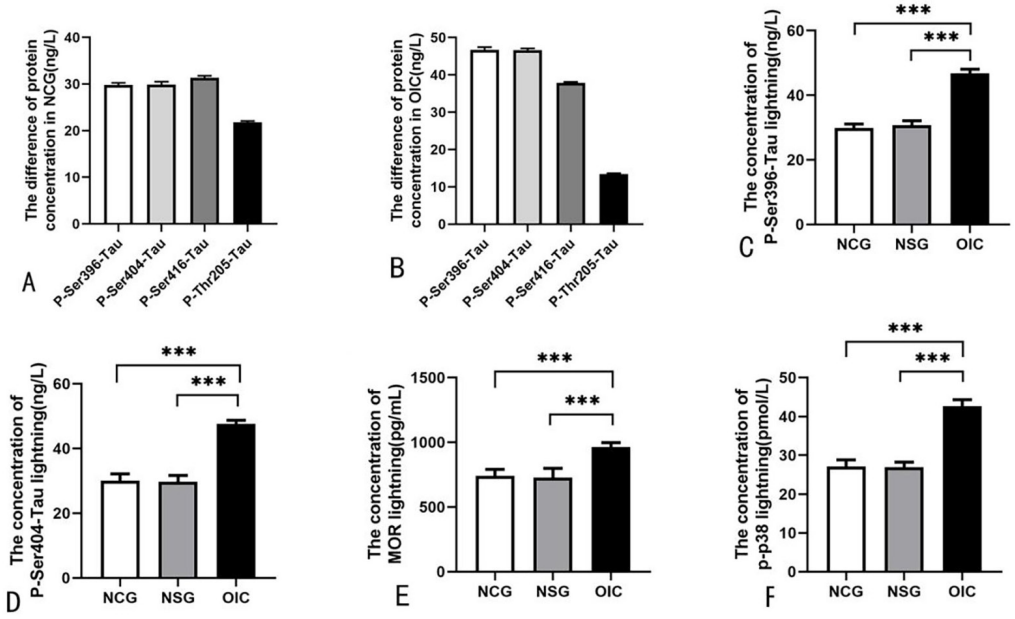

Fig. 4. ELISA of protein content and statistical analysis of colonic muscular layer in the three groups of rats 7 days after modeling. **A** and **B**, comparisons of tau expressions at each phosphorylation site in the distal colonic muscular layer of NCG and OIC rats. **C-F,** the expressions of P-Ser396-Tau, P-Ser404-Tau, MOR and p-p38 were significantly increased in the colonic muscular layer of OIC rats compared with that of NCG and NSG (***$P < 0.001$).

Expressions of Tau-related biomarkers and MOR in the distal colonic muscular and myenteric layer

ELISA showed that tau phosphorylation at Ser396/404/416 was higher in the distal colonic muscular layer of NCG rats while Ser396/404 phosphorylation level was higher in the distal colonic muscular layer of OIC rats, suggesting that the tau phosphorylation at Ser396 and Ser404 might be associated with the occurrence of OIC (Fig. 4A, B). Statistically significant increase in expressions of P-Ser396-Tau, P-Ser404-Tau, MOR and p-p38 levels was found in the distal colonic muscular layer of OIC rats compared with that of NCG and NSG ($^{***}P<0.001$, Fig. 4C, F).

Immunoblotting results indicated that there were no significant changes between the OIC and NCG or NSG rats' distal colonic muscular layers, in terms of Tau and p38 expression levels ($P>0.05$, Fig. 5A, C, D, I). While P-Ser396-Tau, P-Ser404-Tau, MOR, PKC and p-p38 expression were increased significantly in OIC rats than that in either NCG or NSG rats ($^{*}P<0.05$, $^{**}P< 0.01$, Fig. 5A-C, E-H, J).

Effect of different drug intervention on body weight, fecal grade scores, and IPVs of rats

On the 4th day of the imposed intervention, rats in the OIC+Naloxone and OIC+SB203580 groups exhibited an increase in their body weight gaining rates (~10g/day), while rats in the OIC+NaCl and OIC+ANS groups gained body weights at a rate of about 2 g per day (Fig. 6A).

On the 4th day of the intervention, the feces of rats in the OIC+Naloxone and OIC+SB203580 groups appeared in the shape of salami (Fig. 6B), with a grade score of IV in the OIC+Naloxone group, and III in the OIC+SB203580 group (Fig. 6C). In the case of rats of the OIC+NaCl and OIC+ANS groups, feces were scattered as hard lumps (Fig. 6B), and the fecal grade scores for these two groups ranged from I to II (Fig. 6C). On the 4th day of the drug intervention, there were significant differences in the fecal grade scores between the OIC+SB203580 group and OIC+NaCl and OIC+ANS groups ($^{***}P< 0.001$, Fig. 6C).

During an in vivo drug intervention for 4 days, India ink was administered orally to 4 groups of rats once a day and the daily colonic propulsion velocity was measured. Compared with the 3rd day before the drug intervention, there were no significant difference in colonic propulsion velocity in rats of the OIC+NaCl and OIC+ANS groups on the 4th day ($P>0.05$, Fig. 6D, F). However, compared with the 3rd day before the drug intervention, the colonic propulsion velocity of rats in the OIC+Naloxone and OIC+SB203580 groups were significantly increased on

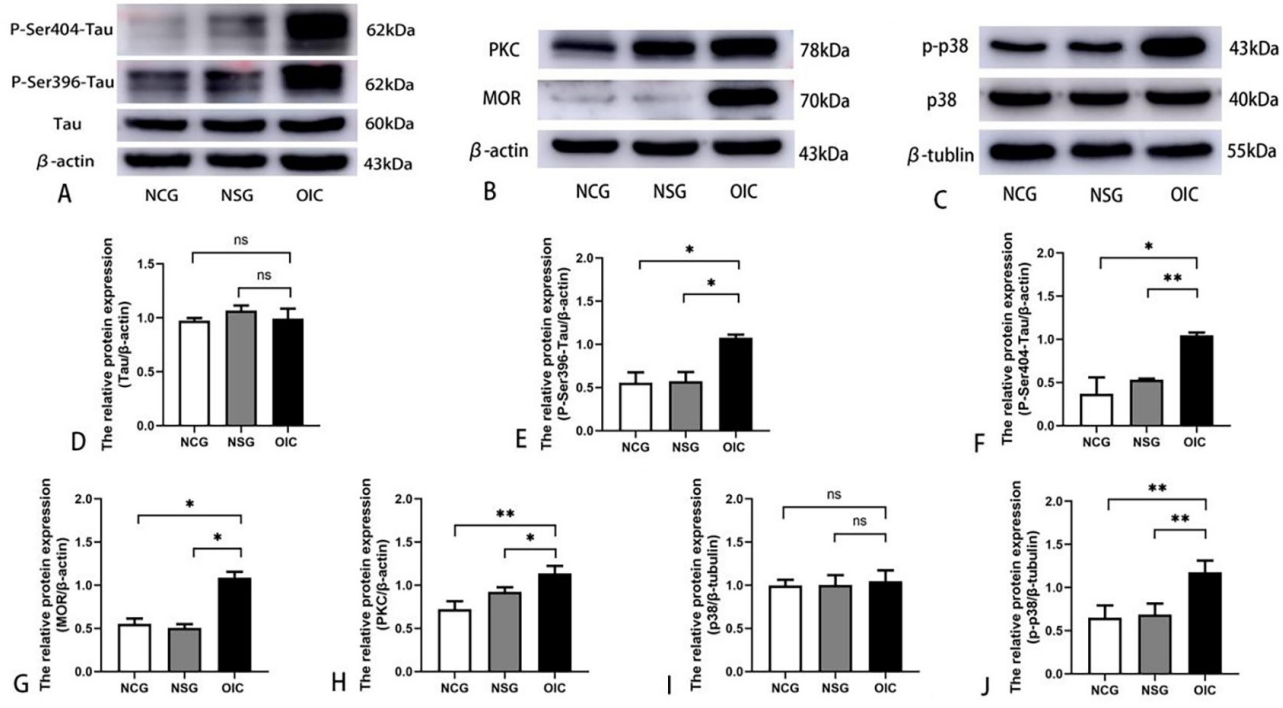

Fig. 5. Expressions of Tau, P-Ser396-Tau P-Ser404-Tau, MOR, PKC, p38 and p-p38 in the distal colonic muscles of three groups of rats on the 7th day of modeling. **A-C,** Protein expressions of Tau, P-Ser396-Tau, P-Ser404-Tau, MOR, PKC, p38 and p-p38. **D-J,** Statistical analysis of Tau, P-Ser396-Tau, P-Ser404-Tau, MOR, PKC, p38 and p-p38 expressions.

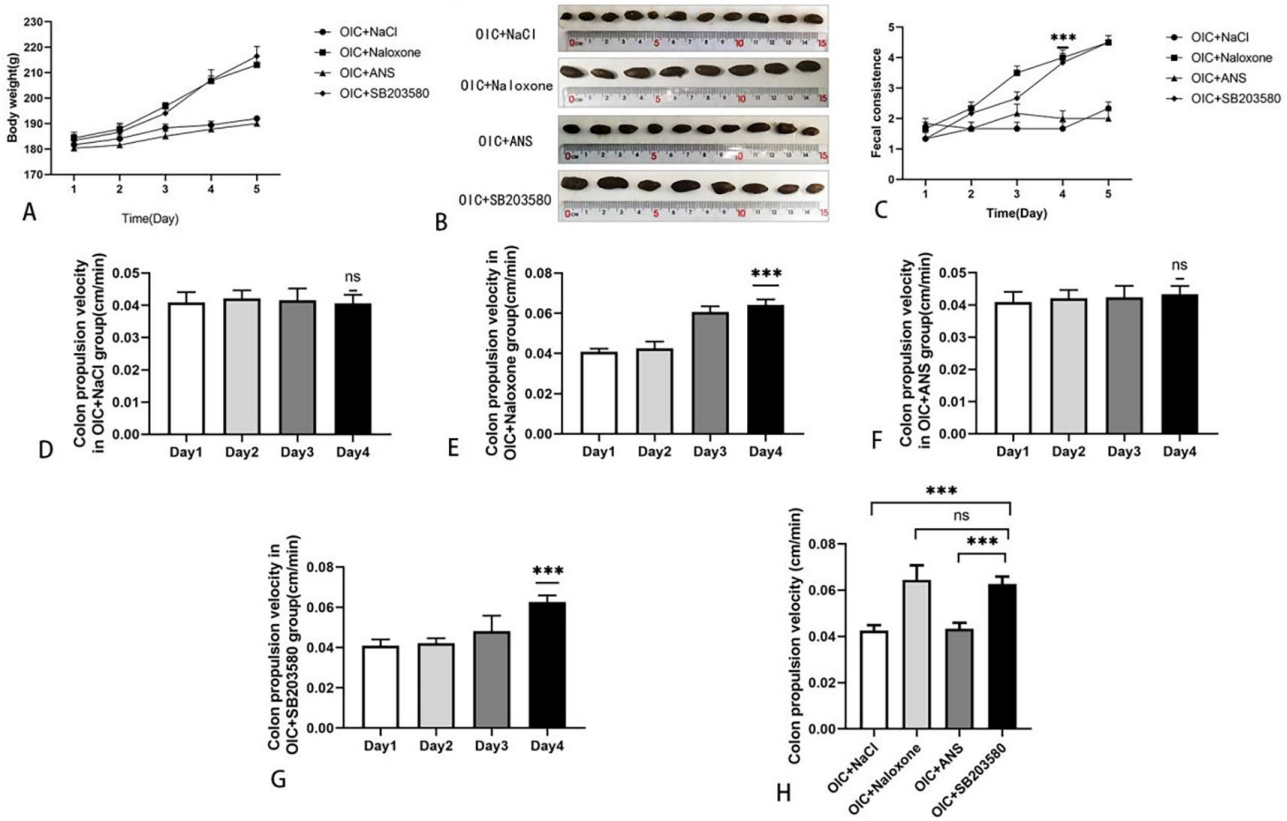

Fig. 6. Comparisons of body weights, fecal trait grade scores of rats and colonic propulsion velocities in the four different groups following the drug intervention *in vivo*. **A,** Changes in the body weight of rats during drug intervention. **B,** Fecal traits of rats on the 4th day of drug intervention. **C,** Comparison of fecal trait grade scores during the drug intervention. **D-G**, Comparison of colonic propulsion velocity in four groups during 4 days of drug intervention. Compared with the 3rd day before drug intervention. **H,** Comparison of colonic propulsion velocities between the four groups of rats on the 4th day after *in vivo* drug intervention.

the 4th day (***P<0.001, Fig. 6E, G). On the 4th day of the administration of Indian ink, rats in the OIC+Naloxone group took about 4.5h for the ink to completely pass out of the colon from the end of the small intestine; The OIC+SB203580 group rats required about 5h, the OIC+NaCl group required about 7.3h and the OIC+ANS group required about 7h. There was no significant difference between the OIC+SB203580 and OIC+Naloxone groups (P>0.05, Fig. 6H); the OIC+SB203580 group exhibited statistically significant increases in the colonic propulsion velocities compared to that of the OIC+NaCl and OIC+ANS groups (***P<0.001, Fig. 6H).

Effect of different drug intervention on expression of Tau-related biomarkers and MOR

Western blot results indicated that on the 4th day of the intervention, the expression levels of Tau, P-Ser396-Tau, P-Ser404-Tau, p38 and p-p38 in the colonic myocardium of rats in the OIC+SB203580 group did not vary significantly compared with those in the OIC+Naloxone group (P>0.05, Fig. 7). There were also no significant differences in the expressions of Tau and p38 in rat colon muscle layers between the OIC+SB203580 and OIC+NaCl or OIC+ANS groups (P>0.05, Fig. 7A, C, F). However, protein levels of P-Ser396-Tau, P-Ser404-Tau and p-p38 were significantly reduced in the OIC+SB203580 group compared with those in the OIC+NaCl and OIC+ANS groups (**P<0.01, Fig. 7A, B, D, E, G).

ELISA results revealed that on the 4th day of the imposed intervention, there was no significant difference in the expression of P-Ser396-Tau, P-Ser404-Tau and p-p38 in the OIC+SB203580 group compared to the OIC+Naloxone group, which was not statistically significant (P>0.05, Fig. 8). However, the levels of P-Ser396-Tau, P-Ser404-Tau and p-p38 expressions were significantly reduced in the OIC+SB203580 group compared with those in the OIC+NaCl and OIC+ANS groups (***P<0.001, Fig. 8).

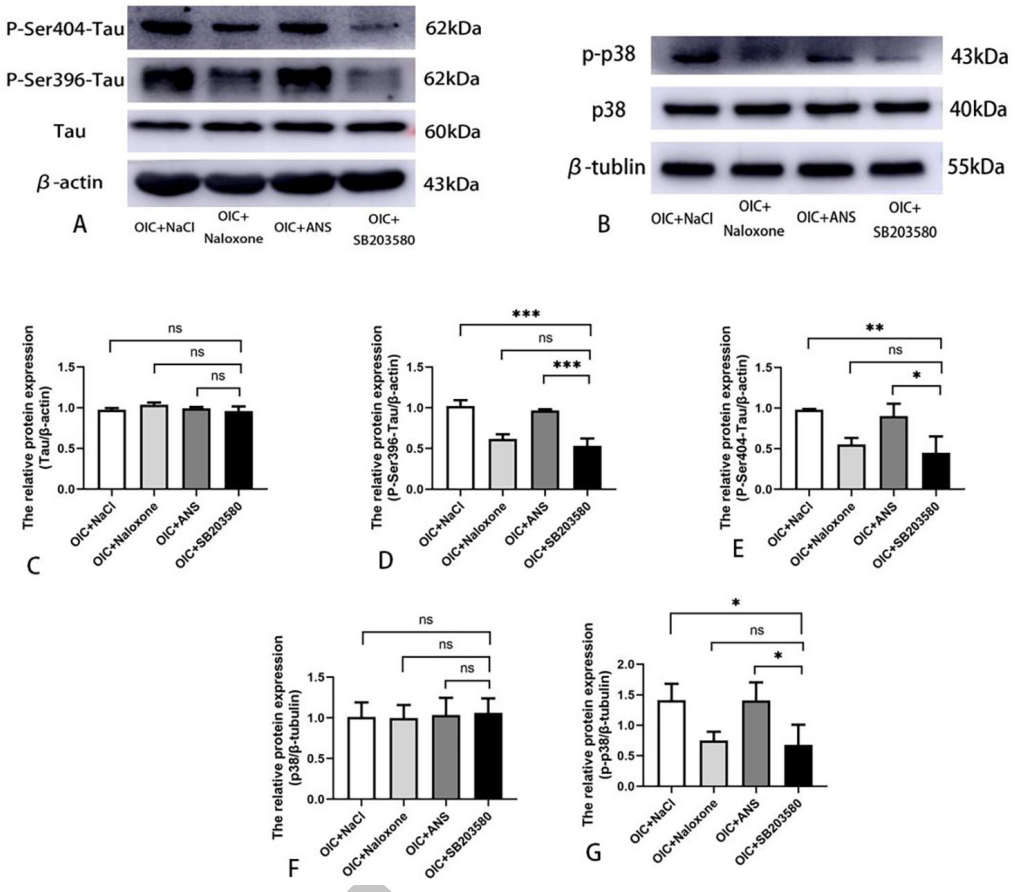

Fig. 7. Changes in the expressions of Tau, P-Ser396-Tau, P-Ser404-Tau, p38 and p-p38 proteins in the distal colonic musculatures of four groups of rats after 4 days of in vivo drug intervention. **A** and **B,** Protein expressions of Tau, P-Ser396-Tau, P-Ser404-Tau, p38 and p-p38. **C-G,** Statistical analysis of Tau, P-Ser396-Tau, P-Ser404-Tau, p38 and p-p38 expressions.

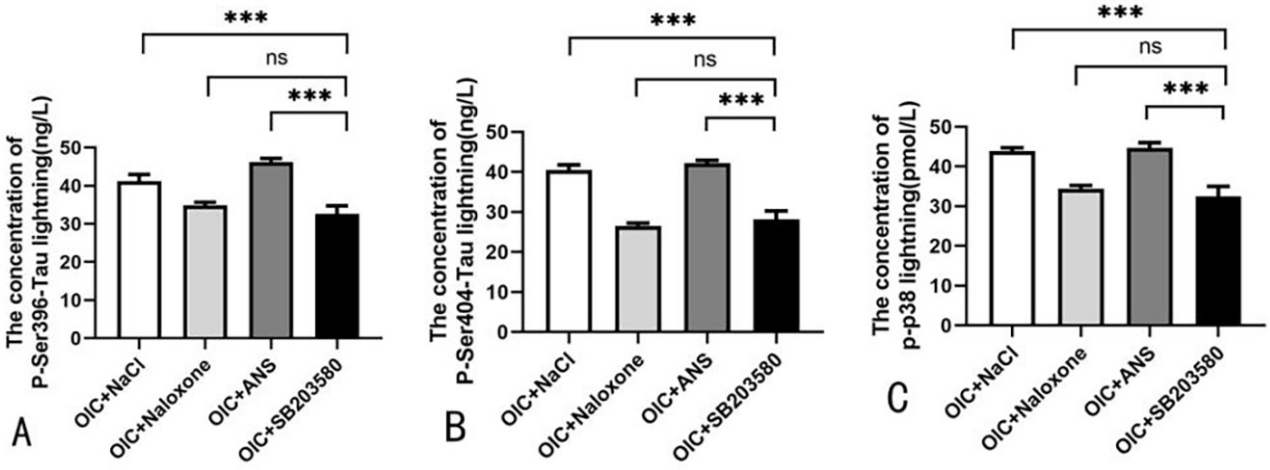

Fig. 8. ELISA detection of protein contents and statistical analysis of colonic muscular layer in the four groups of rats after 4 days of intervention in vivo. **A-C,** On the 4th day of the imposed intervention, expressions of P-Ser396-Tau, P-Ser404-Tau and p-p38 were significantly reduced in the colonic muscular layers of rats in the OIC+SB203580 group compared with those in the OIC+NaCl and OIC+ANS groups (***P<0.001).

DISCUSSION

Opioids, while analgesic, function through their interaction with MORs expressed on the enteric nerve cells (Luo *et al*., 2011). Opioids can effectively reduce GI motility, inhibiting the transmission function of the GI tract, and inducing constipation (Neefjes *et al*., 2019). Therefore, in this study, the MOR-selective agonist Lop was used to produce a rat constipation model for mechanistic investigation of the drug. The model was successfully established, according to the Bristol stool trait scoring guidelines, for the detection of colonic propulsion velocity. The results showed that the propulsion velocity of the proximal, middle, and distal colonic regions in OIC rats was significantly slower, especially in the distal colon. It has been reported that the retention time of intestinal lumen contents in the colon after morphine administration is approximately 80% of the entire GI elimination time (Banta *et al*., 1979). Therefore, the distal colon was the main target of this study.

In the colon, the distribution of MORs is significantly denser than in the stomach and small intestine areas (Lay *et al*., 2016). In the GI tract, MORs show a wide distribution pattern in the nerve cells of the intestinal muscular plexus and is involved in regulating the movement of intestinal smooth muscles, mainly for modulating the release of neurotransmitters, particularly the inhibitory ones (Kurz and Sessler, 2003). Neurotransmitters are mainly synthesized in the nerve cell cytosol and later transported to the termini via axons to participate in neuromodulatory functions at synapses. However, the underlying mechanisms of MOR-mediated regulation of neurotransmitter release from enteric nerve cells are poorly understood.

Studies reveal that morphine is involved in the regulation of tau protein phosphorylation via activation of the JNK/p38 signaling pathway in the CNS neurons after its interaction with MORs (Cao *et al*., 2013). In matured neuronal cells, tau is mainly distributed in axons to maintain the axonal transportation system (Wang and Mandelkow, 2016). Here, IF-based histochemical double labeling showed that Tau, P-Ser396-Tau, P-Ser404-Tau, PKC, p38 and p-p38 were distributed in rat distal colonic muscular plexus neuronal cells, colocalizing with the MOR.

Tau, a microtubule-associated protein, is predominantly found in neurons and is encoded by the *MAPT* gene (Andreadis, 2006). Tau plays a role in promoting microtubule polymerization to form full-length microtubules that bind tightly to the newly polymerized microtubules to prevent their depolymerization and maintain their structural stabilities (Noble *et al*., 2013). In the CNS, tau can be expressed any of these six isoforms by alternative splicing, namely 0N3R, 0N4R, 1N3R, 1N4R, 2N3R and 2N4R (Goedert and Jakes, 1990). In this study, transcriptomic analysis showed that seven different tau-associated mRNAs were expressed after selective splicing of the *MAPT* gene. Of which, three tau isoforms, namely 2N4R, 1N4R and 0N4R, were expressed in the rat distal colonic muscular layers. These results suggest that tau can be distributed in the colonic nerve cells and may have a functional correlation with the MOR.

A low-level phosphorylation state of tau is necessary for its normal physiological functions (Kolarova *et al*., 2012). While excessive phosphorylation of tau reduces its binding to microtubules, resulting in the disintegration and degeneration of neuronal microtubule structure, as observed in certain pathological conditions (Guo *et al*., 2017). Using western blot and ELISA, we showed that levels of pSer396-tau, pSer404-tau, p-p38, and MOR expressions were significantly increased in the distal colonic muscle layers of OIC rats, indicating that MORs could be aberrantly activated to induce tau hyperphosphorylation in the enteric nerve cells.

It has been demonstrated that morphine-activated MORs regulate tau phosphorylation through the JNK/p38 signaling pathway in the CNS (Cao *et al*., 2013). MORs are G-protein-coupled receptors (GPCRs) (Bruchas and Roth, 2016). Upon activation of GPCRs, PLC activation via G protein β and γ subunits catalyzes the hydrolysis of phosphatidylinositol 4,5-bisphosphate (PIP 2) to produce inositol 1,4,5-trisphosphate (IP3) and diacylglycerol (DAG) (Orr *et al*., 1992). This in turn induces the release of Ca2+, which binds to aspartate (Asp) (C2 structural domain of PKC), leading to the exposure of the PIP 2 binding pocket (Newton and Johnson, 1998). the C1B structural domain of PKC binds to the ligand DAG on the plasma membrane, ultimately activating the kinase function of the protein (Orr *et al*., 1992). The activated PKC induces p38 phosphorylation, then leading to tau phosphorylation (Falcicchia *et al*., 2020). Therefore, we hypothesized that the aberrant activation of the MOR in colonic myenteric plexus nerve cells might induce tau hyperphosphorylation through the PKC/p38 signaling pathway, which plays a role in constipation. The results of this study showed that administration of the p38 blocker SB203580 significantly alleviated the symptoms of OIC, with a similar effect to the MOR antagonist naloxone. Clinical studies have suggested that naloxone, although it is able to relieve OIC, can severely affect the GI system inducing cardiovascular and respiratory disorders (Meng and Zheng, 1991). However, the administration of the p38 agonist ANS significantly increased the symptoms of OIC.

The pathological mechanisms of OIC include at

least in part as follows. Firstly, the binding of opioids to peripheral opioid receptors in the submucosal and myenteric plexuses decreases neurotransmitter release which leads to impaired motility (Wang *et al*., 2023). It has been reported that activation of κ-opioid receptor receptors in the ileal could inhibit cholinergic transmission by regulating N-type Ca^{2+} channels (Imam *et al*., 2018). Secondly, the interaction of gut mechanoreceptors and chemoreceptors and μ-opioid receptors activation in the gastrointestinal tract directly affects intestinal circular and longitudinal muscles that promote peristalsis (Imam *et al*., 2018). Thirdly, inflammation and enteric glial cells also participate in the process of OIC. Gao *et al*. (2021) showed that morphine activated enteric glial cells via μ-opioid receptors and increased the release of proinflammatory cytokines, such as TNF-α, IL-1β, and IL-6 (Gao *et al*., 2021). In addition, microbiota also plays a potential role in the mechanism of OIC. Touw *et al*. (2017) show that decreased gut motility alters the gut microbial community and its metabolism, leading to the promotion of the feed-forward loop that slows GI transit time even further, while the reinforcement of the decreased gut motility, in turn, sustains the selective advantage of constipation-associated microbiota (Touw *et al*., 2017). Apart from above the pathological mechanisms of OIC, our study discovers that there is a unique distribution pattern of tau within the distal colonic musculature of OIC rats, and the abnormal activation of MORs contributes to the hyperphosphorylation of tau protein, which in turn induces the development of OIC.

Noticeably, the brain-gut axis in central neurological dysfunction attracts more attention in recent years. Some evidence suggests that misfolded protein aggregates found in the brain of Alzheimer's disease may have a strong association with the gut (Imam *et al*., 2018). Chen *et al*. (2021) argue that colonic infusion of Alzheimer's disease brain extracts, which encompass both Aβ and Tau N368 fibrils, into the gut of young 3xTg mice also travels along the vagus nerve and activates the C/EBPβ/δ-secretase pathway, accelerating Alzheimer's disease-like pathologies in the hippocampus (Chen *et al*., 2021). In our study, we find that there is a unique distribution pattern of tau within the distal colonic musculature of OIC rats, and we infer this finding provides a novel and potential direction for brain-gut axis research.

Currently, there are some deficiencies in the evaluation criteria. Our research group is developing better experimental methods to bridge this gap. Although our research focuses on the correlation between opioid-induced constipation and tau phosphorylation, considering that the content is not rich enough, the research team will add new ideas and experiments in the future to explore more research fields.

CONCLUSION

We demonstrated that MORs might regulate tau function through the PKC/p38 MAPK signaling pathway in the distal colonic muscular layer of rats. After the administration of opioids, MORs were abnormally activated, that induced tau hyperphosphorylation, affecting the axonal stability and transport function, leading to abnormal neurotransmitter release and occurrence of constipation symptoms. We bridge the gap between the tau and nervous system, especially the peripheral system, which lay a theoretical foundation for the potential mechanism of opioid-induced constipation.

DECLARATIONS

Funding

This work was supported by grants from the Nation Natural Science Foundation of China (No.31860275) and the Natural Science Foundation of Ningxia (No.2022AAC02032).

Ethics approval and consent to participate

The experiments were conducted in strict accordance with the Ethical Review of Laboratory Animal Welfare guidelines issued by the General Administration of Quality Supervision, Inspection and Quarantine, and the National Bureau of Standards. Animal experimental operations in our study were performed in accordance with Guide for Animal Care and Use of Ningxia Medical University. Animal experiments were approved by Ethics Committees and Health Authorities of Ningxia Medical University [No.SCXK(Ning)2020-0001].

Availability of data and materials

All data generated or analyzed during this study are included in this published article.

Supplementary material

There is supplementary material associated with this article. Access the material online at: https://dx.doi.org/10.17582/journal.pjz/20230512070544

Statement of conflict of interest

The authors have declared no conflict of interest.

REFERENCES

Andreadis, A., 2006. Misregulation of tau alternative splicing in neurodegeneration and dementia.

Prog. Mol. Subcell. Biol., **44**: 89-107. https://doi.org/10.1007/978-3-540-34449-0_5

Banta, C.A., Clemens, E.T., Krinsky, M.M. and Sheffy, B.E., 1979. Sites of organic acid production and patterns of digesta movement in the gastrointestinal tract of dogs. *J. Nutr.*, **109**: 1592-1600. https://doi.org/10.1093/jn/109.9.1592

Bruchas, M.R. and Roth, B.L., 2016. New technologies for elucidating opioid receptor function. *Trends Pharmacol. Sci.*, **37**: 279-289. https://doi.org/10.1016/j.tips.2016.01.001

Cao, M., Liu, F., Ji, F., Liang, J., Liu, L., Wu, Q. and Wang, T., 2013. Effect of c-Jun N-terminal kinase (JNK)/p38 mitogen-activated protein kinase (p38 MAPK) in morphine-induced tau protein hyperphosphorylation. *Behav. Brain Res.*, **237**: 249-255. https://doi.org/10.1016/j.bbr.2012.09.040

Chen, C., Zhou, Y., Wang, H., Alam, A., Kang, S.S., Ahn, E.H., Liu, X., Jia, J. and Ye, K., 2021. Gut inflammation triggers C/EBPβ/δ-secretase-dependent gut-to-brain propagation of Aβ and Tau fibrils in Alzheimer's disease. *EMBO J.*, **40**: e106320. https://doi.org/10.15252/embj.2020106320

Falcicchia, C., Tozzi, F., Arancio, O., Watterson, D.M. and Origlia, N., 2020. Involvement of p38 MAPK in synaptic function and dysfunction. *Int. J. mol. Sci.*, **21**: 5624. https://doi.org/10.3390/ijms21165624

Farmer, A.D., Holt, C.B., Downes, T.J., Ruggeri, E., Del Vecchio, S. and De Giorgio, R., 2018. Pathophysiology, diagnosis, and management of opioid-induced constipation. *Lancet Gastroenterol. Hepatol.*, **3**: 203-212. https://doi.org/10.1016/S2468-1253(18)30008-6

Galligan, J.J. and Akbarali, H.I., 2014. Molecular physiology of enteric opioid receptors. *Am. J. Gastroenterol. Suppl.*, **2**: 17-21. https://doi.org/10.1038/ajgsup.2014.5

Galligan, J.J. and Sternini, C., 2017. Insights into the role of opioid receptors in the GI Tract: Experimental evidence and therapeutic relevance. *Handb. exp. Pharmacol.*, **239**: 363-378. https://doi.org/10.1007/164_2016_116

Gao, H., Zhang, Y., Li, Y., Chang, H., Cheng, B., Li, N., Yuan, W., Li, S. and Wang, Q., 2021. μ-opioid receptor-mediated enteric glial activation is involved in morphine-induced constipation. *Mol. Neurobiol.*, **58**: 3061-3070. https://doi.org/10.1007/s12035-021-02286-0

Goedert, M. and Jakes, R., 1990. Expression of separate isoforms of human tau protein: Correlation with the tau pattern in brain and effects on tubulin polymerization. *EMBO J.*, **9**: 4225-4230. https://doi.org/10.1002/j.1460-2075.1990.tb07870.x

Guerrero-Alba, R., Valdez-Morales, E.E., Jimenez-Vargas, N.N., Lopez-Lopez, C., Jaramillo-Polanco, J., Okamoto, T., Nasser, Y., Bunnett, N.W., Lomax, A.E. and Vanner, S.J., 2017. Stress activates pronociceptive endogenous opioid signalling in DRG neurons during chronic colitis. *Gut*, **66**: 2121-2131. https://doi.org/10.1136/gutjnl-2016-311456

Guo, T., Noble, W. and Hanger, D.P., 2017. Roles of tau protein in health and disease. *Acta Neuropathol.*, **133**: 665-704. https://doi.org/10.1007/s00401-017-1707-9

Huang, Y.J., Jiang, S.S. and Xiang, Y.F., 2020. Effect of loperamide on the stability of the rat model of slow transit constipation: An experimental study. *Hunan J. Tradit. Chin. Med.*, **36**: 153-156.

Imam, M.Z., Kuo, A., Ghassabian, S. and Smith, M.T., 2018. Progress in understanding mechanisms of opioid-induced gastrointestinal adverse effects and respiratory depression. *Neuropharmacology*, **131**: 238-255. https://doi.org/10.1016/j.neuropharm.2017.12.032

Kolarova, M., García-Sierra, F., Bartos, A., Ricny, J. and Ripova, D., 2012. Structure and pathology of tau protein in Alzheimer disease. *Int. J. Alzheimers Dis.*, **2012**: 731526. https://doi.org/10.1155/2012/731526

Kurz, A. and Sessler, D.I., 2003. Opioid-induced bowel dysfunction: Pathophysiology and potential new therapies. *Drugs*, **63**: 649-671. https://doi.org/10.2165/00003495-200363070-00003

Lauretti, E. and Praticò, D., 2020. Alzheimer's disease: Phenotypic approaches using disease models and the targeting of tau protein. *Expert. Opin. Ther. Targets*, **24**: 319-330. https://doi.org/10.1080/14728222.2020.1737012

Lay, J., Carbone, S.E., DiCello, J.J., Bunnett, N.W., Canals, M. and Poole, D.P., 2016. Distribution and trafficking of the μ-opioid receptor in enteric neurons of the guinea pig. *Am. J. Physiol. Gastrointest. Liver Physiol.*, **311**: G252-266. https://doi.org/10.1152/ajpgi.00184.2016

Luo, M., Li, L., Lu, C.Z. and Cao, W.K., 2011. Clinical efficacy and safety of lactulose for minimal hepatic encephalopathy: A meta-analysis. *Eur. J. Gastroenterol. Hepatol.*, **23**: 1250-1257. https://doi.org/10.1097/MEG.0b013e32834d1938

Ma, L., Qu, Z., Xu, L., Han, L., Han, Q., He, J., Luan, X., Wang, B., Sun, Y. and He, B., 2021. 7, 8-dihydroxyflavone enhanced colonic cholinergic contraction and relieved loperamide-induced

constipation in rats. *Dig. Dis. Sci*., **66**: 4251-4262. https://doi.org/10.1007/s10620-020-06817-y

Meng, Q.X. and Zheng, S.J., 1991. Application of naloxone to antagonize cardiovascular adverse reactions induced by narcotic analgesics. *Foreign Med. Anesth. Resusc*., **12**: 371-373.

Neefjes, E.C.W., van der Wijngaart, H., van der Vorst, M.J.D.L., Ten Oever, D., van der Vliet, H.J., Beeker, A., Rhodius, C.A., van den Berg, H.P., Berkhof, J., Verheul, H.M.W., 2019. Optimal treatment of opioid induced constipation in daily clinical practice. An observational study. *BMC Palliat. Care*, **18**: 31. https://doi.org/10.1186/s12904-019-0416-7

Newton, A.C. and Johnson, J.E., 1998. Protein kinase C: A paradigm for regulation of protein function by two membrane-targeting modules. *Biochim. biophys. Acta*, **1376**: 155-172. https://doi.org/10.1016/S0304-4157(98)00003-3

Noble, W., Hanger, D.P., Miller, C.C. and Lovestone, S., 2013. The importance of tau phosphorylation for neurodegenerative diseases. *Front. Neurol*., **4**: 83. https://doi.org/10.3389/fneur.2013.00083

Ohene-Nyako, M., Nass, S.R., Hahn, Y.K., Knapp, P.E. and Hauser, K.F., 2021. Morphine and HIV-1 Tat interact to cause region-specific hyperphosphorylation of tau in transgenic mice. *Neurosci. Lett*., **741**: 135502. https://doi.org/10.1016/j.neulet.2020.135502

Orr, J.W., Keranen, L.M. and Newton, A.C., 1992. Reversible exposure of the pseudo substrate domain of protein kinase C by phosphatidylserine and diacylglycerol. *J. biol. Chem*., **267**: 15263-15266. https://doi.org/10.1016/S0021-9258(19)49525-2

Porta-Sales, J., Nabal-Vicuna, M., Vallano, A., Espinosa, J., Planas-Domingo, J., Verger-Fransoy, E., Julià-Torras, J., Serna, J., Pascual-López, A., Rodríguez, D., Grimau, I., Morlans, G., Sala-Rovira, C., Calsina-Berna, A., Borras-Andrés, J.M. and Gomez-Batiste, X., 2015. Have we improved pain control in cancer patients? A multicenter study of ambulatory and hospitalized cancer patients. *J. Palliat. Med*., **18**: 923-932. https://doi.org/10.1089/jpm.2015.29002.jps

Pourtalebi, J.L., Sasanipour, Z. and Azadi, A., 2018. Promising horizon to alleviate Alzeheimer's disease pathological hallmarks via inhibiting mTOR signaling pathway: A new application for a commonplace analgesic. *Med. Hypoth*., **110**: 120-124. https://doi.org/10.1016/j.mehy.2017.12.007

Ramage, S.N., Anthony, I.C., Carnie, F.W., Busuttil, A., Robertson, R. and Bell, J.E., 2005. Hyperphosphorylated tau and amyloid precursor protein deposition is increased in the brains of young drug abusers. *Neuropathol. appl. Neurobiol*., **31**: 439-448. https://doi.org/10.1111/j.1365-2990.2005.00670.x

Touw, K., Ringus, D.L., Hubert, N., Wang, Y., Leone, V.A., Nadimpalli, A., Theriault, B.R., Huang, Y.E., Tune, J.D., Herring, P.B., Farrugia, G., Kashyap, P.C., Antonopoulos, D.A. and Chang, E.B., 2017. Mutual reinforcement of pathophysiological host-microbe interactions in intestinal stasis models. *Physiol. Rep*., **5**: e13182. https://doi.org/10.14814/phy2.13182

Wang, L., Gharibani, P., Yang, Y., Guo, Y. and Yin, J., 2023. Regulation of enteric nervous system via sacral nerve stimulation in opioid-induced constipated rats. *Front. Neurosci*., **17**: 1146883. https://doi.org/10.3389/fnins.2023.1146883

Wang, Y. and Mandelkow, E., 2016. Tau in physiology and pathology. *Nat. Rev. Neurosci*., **17**: 5-21. https://doi.org/10.1038/nrn.2015.1

Wang, Y., 2021. Progress in pathological mechanism and therapy of opioid-induced constipation. *Chin. J. clin. Oncol*., **48**: 852-857.

Young, A., Viswanath, A., Kalladka, M., Khan, J., Eliav, E. and Diehl, S.R., 2018. Mouse model demonstrates strain differences in susceptibility to opioid side effects. *Neurosci. Lett*., **675**: 110-115. https://doi.org/10.1016/j.neulet.2018.03.022

Zhang, B., Yao, Y., Cornec, A.S., Oukoloff, K., James, M.J., Koivula, P., Trojanowski, J.Q., Smith, A.B., Lee, V.M., Ballatore, C. and Brunden, K.R., 2018. A brain-penetrant triazolopyrimidine enhances microtubule-stability, reduces axonal dysfunction and decreases tau pathology in a mouse tauopathy model. *Mol. Neurodegener*., **13**: 59. https://doi.org/10.1186/s13024-018-0291-3

Pakistan J. Zool., pp 1-13, 2023. **DOI**: https://dx.doi.org/10.17582/journal.pjz/20230512070544

Supplementary Material

Modulation of Tau Expression in the Colonic Muscle Layer of a Rat Model with Opioid-Induced Constipation

Jinzhao Li[1], Yawen Zhang[2], Binghan Jia[1], Yuqiong Zhao[1], Huijuan Luo[1], Xiaojie Ren[1], Yuan Li[3], Xiaoyan Bai[1], Jing Ye[3] and Junping Li[1]*

[1]Department of College of Basic Medical Sciences, Ningxia Medical University, No. 1160 of Shengli Street, Ningxia Hui Autonomous Region, Yinchuan 750004, China
[2]Department of General Surgery, People's Hospital of Ningxia Hui Autonomous Region, Yinchuan 750004, China
[3]Department of College of Clinical Medicine, Ningxia Medical University, Yinchuan 750004, China

Jinzhao Li and Yawen Zhang contributed equally to this study.

Supplementary Material 1. Material methods of the gene sequencing.

Experiment protocol

1ug total RNA was prepared for cDNA libraries using cDNA-PCR Sequencing Kit (SQK-PCS109) protocol provided by Oxford Nanopore Technologies (ONT). Briefly, the template switching activity of reverse transcriptases enrich for full-length cDNAs and add defined PCR adapters directly to both ends of the first-strand cDNA. And following cDNA PCR for 14 circles with LongAmp Tag (NEB). The PCR products were then subjected to ONT adaptor ligation using T4 DNA ligase (NEB). Agencourt XP beads was used for DNA purification according to ONT protocol. The final cDNA libraries were added to FLO-MIN109 flowcells and run on PromethION platform at Biomarker Technology Company (Beijing, China).

Data analysis

Oxford nanopore technologies long read processing

Raw reads were first filtered with minimum average read quality score=7 and minimum read length=500bp. Ribosomal RNA were discarded after mapping to rRNA database. Next, full-length, non-chemiric (FLNC) transcripts were determined by searching for primer at both ends of reads. Clusters of FLNC transcripts were obtained after mapping to reference genome with mimimap2, and consensus isoforms were obtained after polishing within each cluster by pinfish.

Remove redundant

Consensus sequences were mapped to reference genome using minimap2. Mapped reads were further collapsed by cDNA_Cupcake package with min-coverage=85% and min-identity=90%. 5' difference was not considered when collapsing redundant transcripts.

Find fusion transcript

The criteria for fusion candidates are that a single transcript must:

(1) must map to 2 or more loci

(2) minimum coverage for each loci is 5% and minimum coverage in bp is >= 1 bp

(3) total coverage is >= 95%

(4) distance between the loci is at least 10kb

Structure analysis

Transcripts were validated against known reference transcript annotations with gffcompare. AS events including IR, ES, AD, AA and MEE were identified by the AStalavista tool. SSR of the transcriptome were identified using MISA. APA analysis was conducted with TAPIS. CDS were predicted by Trans Decoder.

* Corresponding author: lijunping_jp@163.com
0030-9923/2023/0001-0001 $ 9.00/0

Transcription factors prediction

Plant transcription factors were identified with iTAK, while Animal transcription factors were identified from animal TFDB.

lncRNA analysis

Four computational approaches include CPC/CNCI/CPAT/Pfam/ were combined to sort non-protein coding RNA candidates from putative protein-coding RNAs in the transcripts. Putative protein-coding RNAs were filtered out using a minimum length and exon number threshold . Transcripts with lengths more than 200 nt and have more than two exons were selected as lncRNA candidates and further screened using CPC/CNCI/CPAT/Pfam that have the power to distinguish the protein-coding genes from the non-coding genes.

Gene functional annotation

Gene function was annotated based on the following databases:

NR (NCBI non-redundant protein sequences); Pfam (Protein family); KOG/COG/eggNOG (Clusters of Orthologous Groups of proteins); Swiss-Prot (A manually annotated and reviewed protein sequence database);

KEGG (Kyoto Encyclopedia of Genes and Genomes); GO (Gene Ontology).

Quantification of gene/transcript expression levels and Differential expression analysis

Full length reads were mapped to the reference transcriptome sequence. Reads with match quality above 5 were further used to quantify. Expression levels were estimated by reads per gene/transcript per 10,000 reads mapped.

For the samples with biological replicates

Differential expression analysis of two conditions/ groups was performed using the edgeR R package (3.8.6). edgeR provides statistical routines for determining differential expression in digital gene expression data using a model based on the negative binomial distribution. The resulting P values were adjusted using the Benjamini and Hochberg's approach for controlling the false discovery rate. Genes with a P value < 0.05 and foldchange ≥ 1.5 found by edgeR were assigned as differentially expressed.

For the samples without biological replicates

Prior to differential gene expression analysis, for each sequenced library, the read counts were adjusted by edgeR program package through one scaling normalized factor. Differential expression analysis of two samples was performed using the EBSeq R package (1.6.0). The resulting FDR (false discovery rate) were adjusted using the PPDE (posterior probability of being DE). The FDR < 0.05 and foldchange ≥ 1.5 was set as the threshold for significantly differential expression.

Functional enrichment analysis

GO enrichment analysis

Gene Ontology (GO) enrichment analysis of the differentially expressed genes (DEGs) was implemented by the GOseq R packages based Wallenius non-central hyper-geometric distribution (Young et al, 2010), which can adjust for gene length bias in DEGs.

KEGG pathway enrichment analysis

KEGG (Kanehisa et al., 2008) is a database resource for understanding high-level functions and utilities of the biological system, such as the cell, the organism and the ecosystem, from molecular-level information, especially large-scale molecular datasets generated by genome sequencing and other high-throughput experimental technologies (http://www.genome.jp/kegg/). We used KOBAS (Mao et al., 2005) software to test the statistical enrichment of differential expression genes in KEGG pathways.

PPI (Protein protein interaction)

The sequences of the DEGs were blast (blastx) to the genome of a related species (the protein protein interaction of which exists in the STRING database: http://string-db.org/) to get the predicted PPI of these DEGs. Then the PPI of these DEGs were visualized in Cytoscape (Shannon et al., 2003).